ELSEVIER

Chemical Engineering Journal 82 (2001) 209–218

Chemical Engineering Journal

www.elsevier.com/locate/cej

Degradation kinetics of 2,4-D in water employing hydrogen peroxide and UV radiation

Orlando M. Alfano, Rodolfo J. Brandi, Alberto E. Cassano*

INTEC, Instituto de Desarrollo Tecnológico para la Industria Química

Universidad Nacional del Litoral (UNL) and CONICET Güemes 3450, 3000 Santa Fe, Argentina

Accepted 13 October 2000

Abstract

This paper reports the photooxidation of 2,4-dichlorophenoxyacetic acid (2,4-D) in aqueous solution employing hydrogen peroxide and ultraviolet radiation. A kinetic model to represent the degradation of 2,4-D and that of equally toxic intermediate products, such as 2,4-dichlorophenol (DCP) and chlorohydroquinone (CHQ), is presented. The model includes the parallel, direct photolysis of 2,4-D and the most important reaction intermediates. The experimental work was performed in a batch, well-stirred tank reactor irradiated from its bottom using a low power, germicidal, tubular lamp placed at the focal axis of a cylindrical reflector of parabolic cross-section. Herbicide degradation initial rates twenty times faster than those obtained employing UV radiation alone were found. In order to reach more useful conclusions about the ability of the process to reduce the contamination to innocuous final products, simultaneous measurements of the total organic carbon (TOC) were performed. By application of the kinetic model to the whole set of concentration versus time experimental data, the values of the kinetic parameters were obtained. The model permits a good representation of the reaction evolution in a rather wide range of 2,4-D and H_2O_2 initial concentrations.

Keywords: Advanced oxidation technologies; Ultraviolet radiation; Hydrogen peroxide; 2,4-Dichlorophenoxyacetic acid; Degradation; Reaction kinetics

1. Introduction

Conventional methods employed to remove small concentrations of organic pollutants in ground water or industrial effluents, such as air stripping or adsorption by activated carbon, are not good alternatives for contaminants having low volatility or poor adsorption properties. Additionally, these methods only transfer the pollutant from one phase to the other leaving the problem only partially solved. Conversely, effective oxidative treatments lead to the complete mineralization of a great variety of organic substances. Some of these detoxification methods employ strong oxidants such as hydrogen peroxide or ozone combined with one activation step initiated by UV radiation. They are recognized as some of the alternatives offered by the so-called advanced oxidation technologies (AOT). Essentially, these technologies are the result of the strong oxidative properties of $OH^{\bullet}$ radicals thus generated.

The UV/H_2O_2 process has some advantages with respect to the UV/O_3 system. Ozone is not a stable gas and must be generated in situ. Moreover, good ozone gas-to-liquid water mass transfer requires the use of efficient contacting devices. Hydrogen peroxide is easier to transport and store and its oxidative properties are equivalent to those of ozone. Considering at the same time that: (i) H_2O_2 has almost infinite solubility in water; (ii) it does not contains halogens or metals; (iii) the capital cost for installation is lower; and (iv) the operating costs are smaller, this process looks as a better alternative [1,2].

In the UV/H_2O_2 process, radiation having wavelength shorter than 300 nm transforms hydrogen peroxide into $OH^{\bullet}$ radicals, but very often radiation of these wavelengths acts directly and simultaneously on the organic compounds. The oxidative potential of the $OH^{\bullet}$ is very high (2.8 V), only lower than fluorine [2,3]. Complementarily, parallel direct activation of the organic molecule may produce from direct dissociation to the formation of organic radicals or other intermediate compounds. Hence, providing enough H_2O_2 concentration (usually above the stoichiometric demand) and sufficient reaction time, the vast majority of the organic compounds may be transformed into CO_2 and H_2O [4]. There exist many reports on the use of these reactions for degrading aliphatic and aromatic compounds as indicated by the review published by Luñak and Sedlák [5].

* Corresponding author. Tel.: +54-342-4559175; fax: +54-342-4559185.
E-mail address: acassano@alpha.arcride.edu.ar (A.E. Cassano).

1385-8947/01/$ – see front matter
PII: S1385-8947(00)00358-2

Nomenclature

$\boldsymbol{A}$	matrix defined in Eqs. (14) and (15)
$\boldsymbol{B}$	matrix defined in Eqs. (14) and (15)
C	molar concentration (mol m^{-3})
e^a	LVRPA (einstein s^{-1} m^{-3})
G_W	incident radiation at the wall (einstein s^{-1} m^{-2})
h	Planck's constant (J s)
k	kinetic constant, varies with the reaction order
r	H_2O_2/2,4-D initial molar ratio, dimensionless; also radial coordinate (m)
R	reaction rate (mol s^{-1} m^{-3})
t	time (s)
V	volume (m^3)
$\boldsymbol{x}$	position vector (m)
y	Cartesian coordinate (m); also height along the y-coordinate (m)

Greek letters

α	molar absorptivity (m^2 mol^{-1})
β	cylindrical coordinate (rad)
κ	absorption coefficient (m^{-1})
λ	wavelength (nm)
ν	frequency (s^{-1})
ϕ	primary quantum yield (mol einstein^{-1})
Φ	direct photolysis quantum yield (mol einstein^{-1})

Subscripts

CHQ	chlorohydroquinone
D	2,4-dichlorophenoxyacetic acid (2,4-D)
DCP	2,4-dichlorophenol
HA	humic acids
i	relative to species (i)
irr	relative to irradiated volume
L	relative to liquid phase or the liquid phase volume
P	hydrogen peroxide
P1	hydrogen peroxide: linear dependence with respect to the LVRPA
P2	hydrogen peroxide: square root dependence with respect to the LVRPA
T	denotes total value

Special Symbols

$\langle\rangle$	denotes average value

Pichat et al. [6] published a comparative experimental study dealing with different processes to degrade 2,4-D using: (i) titanium dioxide with UV radiation; (ii) hydrogen peroxide and UV radiation; and (iii) direct photolysis, reporting different degradation paths for each one of the reacting systems. They suggested that a combination of them could be the best choice. Other authors [7,8] also studied the degradation of different pollutants in water — 2,4-D among them — using H_2O_2 plus UV changing the initial hydrogen peroxide/organic compound concentration ratio. In all cases, total mineralization was obtained. These contributions were mainly concerned with proving the feasibility of these reactions for pollutant degradation and to propose possible reactions pathways for the oxidative mechanism that produced the mineralization of the involved organic compounds. No quantitative information on the corresponding reaction model and/or kinetic parameters has been published.

In this work, we report a kinetic study of the 2,4-D degradation in the presence of hydrogen peroxide and low wavelength, monochromatic UV irradiation. More precisely, an experimental study on the effects produced on the reaction rates, by the addition of hydrogen peroxide to the photolytic degradation of 2,4-D. Having to deal with two parallel reactions, we first carried out this research employing no hydrogen peroxide, i.e. the direct photolysis was investigated first [9]. Presently, we develop a kinetic model to describe the degradation of 2,4-D in water employing hydrogen peroxide and UV radiation and the kinetic parameters of the reaction rate were obtained from the complete set of concentration versus time experimental data. These results should be of direct application to scaling-up studies because with the proposed methodology the obtained reaction kinetic constants are independent of the reactor size, shape and configuration.

2. The kinetic model

Several studies in the past have proposed different reaction mechanisms for the photolysis of hydrogen peroxide [10–12]. It is widely accepted that the main interactions between hydrogen peroxide with UV radiation and free radicals are well represented by reactions (1)–(6) in Table 1, while reactions (7) and (8) correspond to the decomposition of any of organic compounds existing in the system by reaction with the generated free radicals [1]. Fig. 1 shows the main reaction paths proposed for the 2,4-D photodegradation, where the principal reaction intermediates are chlorohydroquinone, 2,4-dichlorophenol and humic

Table 1
Reaction mechanism[a]

Initiation:	$H_2O_2 \xrightarrow{\Phi_P} 2OH^\bullet$	(1)
Propagation:	$H_2O_2 + OH^\bullet \xrightarrow{k_2} HO_2^\bullet + H_2O$	(2)
	$H_2O_2 + HO_2^\bullet \xrightarrow{k_3} OH^\bullet + H_2O + O_2$	(3)
Termination:	$2OH^\bullet \xrightarrow{k_4} H_2O_2$	(4)
	$2HO_2^\bullet \xrightarrow{k_5} H_2O_2 + O_2$	(5)
	$OH^\bullet + HO_2^\bullet \xrightarrow{k_6} H_2O + O_2$	(6)
Decomposition:	$RH + OH^\bullet \xrightarrow{k_7} \text{products}$	(7)
	$RH + HO_2^\bullet \xrightarrow{k_8} \text{products}$	(8)

[a] In this table, RH represents 2,4-D, CHQ and DCP.

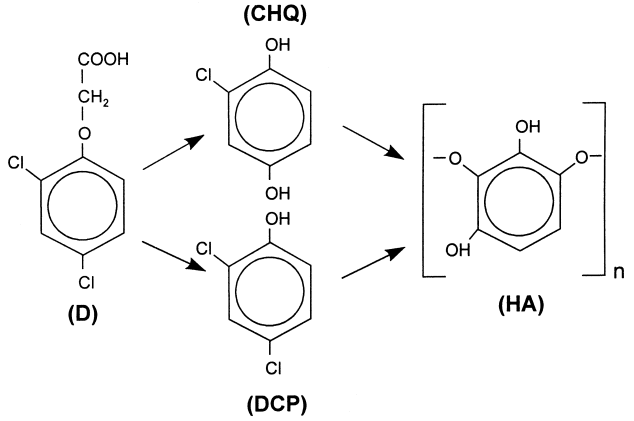

Fig. 1. Main reaction paths for the 2,4-dichlorophenoxyacetic acid photodegradation. Keys: 2,4-D (2,4-dichlorophenoxyacetic acid); DCP (2,4-dichlorophenol); CHQ (chlorohydroquinone).

acids (these last, poorly defined compounds are usually natural components of river waters and hence, considered nontoxic).

A kinetic model was developed that can account for the reaction rates of 2,4-D (D), 2,4-dichlorophenol (DCP), chlorohydroquinone (CHQ), and hydrogen peroxide (P). We have considered the following assumptions: (i) the steady-state approximation may be applied for highly reactive intermediates such as $OH^{\bullet}$ and $HO_2^{\bullet}$ radicals; (ii) the reaction between the organic compounds and $OH^{\bullet}$ and $HO_2^{\bullet}$ free radicals is very fast; and (iii) for formulating the reaction rate of the $HO_2^{\bullet}$ radicals, radical–radical termination reactions are neglected as compared with the propagation reactions. With these assumptions, it can be shown that the hydrogen peroxide reaction rate is given by:

$$R_{\mathrm{P}}(\boldsymbol{x},t) = -k_{\mathrm{P1}}e^a_{\mathrm{P}}(\boldsymbol{x},t) - k_{\mathrm{P2}}C_{\mathrm{P}}(t)[e^a_{\mathrm{P}}(\boldsymbol{x},t)]^{1/2} \tag{9}$$

where k_{P1} and k_{P2} are lumped kinetic constants and $e^a_{\mathrm{P}}(\boldsymbol{x},t)$ the local volumetric rate of photon absorption (LVRPA) by hydrogen peroxide. The kinetic constants k_{P1} and k_{P2} are given by the following expressions:

$$k_{\mathrm{P1}} = \frac{k_2k_3k_6\phi_{\mathrm{P}}}{k_4k_3^2 + k_5k_2^2 + k_6k_2k_3} \tag{10}$$

$$k_{\mathrm{P2}} = \frac{2k_2k_3(\phi_{\mathrm{P}})^{1/2}}{(k_4k_3^2 + k_5k_2^2 + k_6k_2k_3)^{1/2}} \tag{11}$$

For the case of the stable species (i) (i = D, DCP and CHQ) we have the following reaction rates:

$$R_{\mathrm{i}}(\boldsymbol{x},t) = -k_{\mathrm{i,j}}C_{\mathrm{i}}(t)[e^a_{\mathrm{P}}(\boldsymbol{x},t)]^{1/2} \tag{12}$$

where $k_{\mathrm{i,j}}$ (with i, j = D, DCP; D, CHQ; DCP, HA; CHQ, HA) is given by:

$$k_{\mathrm{i,j}} = \frac{(k_{7,(\mathrm{i,j})}k_3 + k_{8,(\mathrm{i,j})}k_2)(\phi_{\mathrm{P}})^{1/2}}{(k_4k_3^2 + k_5k_2^2 + k_6k_2k_3)^{1/2}} \tag{13}$$

Finally, considering the two parallel reactions (Fig. 1), the following kinetic expressions can be written:

$$\begin{bmatrix} R_{\mathrm{D}} \\ R_{\mathrm{DCP}} \\ R_{\mathrm{CHQ}} \\ R_{\mathrm{P}} \end{bmatrix} = \begin{bmatrix} -(\Phi_{\mathrm{D,DCP}} & & & \\ +\Phi_{\mathrm{D,CHQ}}) & 0 & 0 & 0 \\ \Phi_{\mathrm{D,DCP}} & -\Phi_{\mathrm{DCP}} & 0 & 0 \\ \Phi_{\mathrm{D,CHQ}} & 0 & -\Phi_{\mathrm{CHQ}} & 0 \\ 0 & 0 & 0 & -k_{\mathrm{P1}} \end{bmatrix} \times \begin{bmatrix} e^a_{\mathrm{D}} \\ e^a_{\mathrm{DCP}} \\ e^a_{\mathrm{CHQ}} \\ e^a_{\mathrm{P}} \end{bmatrix} + \begin{bmatrix} 0\ 0\ 0 & -C_{\mathrm{D}}k_{\mathrm{D,DCP}} - C_{\mathrm{D}}k_{\mathrm{D,CHQ}} \\ 0\ 0\ 0 & C_{\mathrm{D}}k_{\mathrm{D,DCP}} - C_{\mathrm{DCP}}k_{\mathrm{DCP,HA}} \\ 0\ 0\ 0 & C_{\mathrm{D}}k_{\mathrm{D,CHQ}} - C_{\mathrm{CHQ}}k_{\mathrm{CHQ,HA}} \\ 0\ 0\ 0 & -C_{\mathrm{P}}k_{\mathrm{P2}} \end{bmatrix} \times \begin{bmatrix} (e^a_{\mathrm{D}})^{1/2} \\ (e^a_{\mathrm{DCP}})^{1/2} \\ (e^a_{\mathrm{CHQ}})^{1/2} \\ (e^a_{\mathrm{P}})^{1/2} \end{bmatrix} \tag{14}$$

where e^a_{i} is the LVRPA, Φ_{i} the direct photolysis quantum yield, and k_{P1}, k_{P2} and $k_{\mathrm{i,j}}$ the kinetic parameters corresponding to the H_2O_2/UV reaction. Eq. (14) provides reaction rates for each of the main stable reactant and intermediate species. It should be noted that Eq. (14) for the four reacting species can be written by using the following matrix representation:

$$\boldsymbol{R} = \boldsymbol{A}\boldsymbol{e}^a_{\mathrm{linear}} + \boldsymbol{B}\boldsymbol{e}^a_{\mathrm{square\ root}} \tag{15}$$

Note that humic acids are not well-defined compounds. They represent a family of different polymeric chains resulting from condensation of polyphenols. This uncertainness is also translated into the proper measurement of its optical properties, something that is always important in any photochemical process.

2.1. Limiting cases for the hydrogen peroxide reaction rate

Rearranging Eq. (9), the reaction rate for the hydrogen peroxide species will be:

$$R_{\mathrm{P}}(\boldsymbol{x},t) = -k_{\mathrm{P2}}C_{\mathrm{P}}(t)\left[e^a_{\mathrm{P}}(\boldsymbol{x},t)\right]^{1/2}\left\{\frac{k_{\mathrm{P1}}}{k_{\mathrm{P2}}}\frac{[e^a_{\mathrm{P}}(\boldsymbol{x},t)]^{1/2}}{C_{\mathrm{P}}(t)} + 1\right\} \tag{16}$$

From Eq. (16), the following limiting cases may be obtained:

Case 1 (low LVRPA):

$$\frac{k_{\mathrm{P1}}}{k_{\mathrm{P2}}}\frac{[e^a_{\mathrm{P}}(\boldsymbol{x},t)]^{1/2}}{C_{\mathrm{P}}(t)} \ll 1 \tag{17}$$

Then, the hydrogen peroxide reaction rate will be:

$$R_{\mathrm{P}}(\boldsymbol{x},t) = -k_{\mathrm{P2}}C_{\mathrm{P}}(t)[e^a_{\mathrm{P}}(\boldsymbol{x},t)]^{1/2} \tag{18}$$

Case 2 (high LVRPA):

$$\frac{k_{\mathrm{P1}}}{k_{\mathrm{P2}}}\frac{[e^a_{\mathrm{P}}(\boldsymbol{x},t)]^{1/2}}{C_{\mathrm{P}}(t)} \gg 1 \tag{19}$$

Then, the reaction rate will have the following expression:

$$R_{\mathrm{P}}(\boldsymbol{x}, t) = -k_{\mathrm{P1}} e^a_{\mathrm{P}}(\boldsymbol{x}, t) \tag{20}$$

In the light of these results, the kinetic representation given by Eq. (9) exhibits the following reaction features: (1) for rather low photon absorption rates, the hydrogen peroxide reaction rate is directly proportional to: (i) the hydrogen peroxide concentration and (ii) the square root of the LVRPA, and (2) when the photon absorption rate is high, the reaction rate: (i) is directly proportional to the LVRPA and (ii) shows zero-order dependence with respect to the hydrogen peroxide concentration. This single kinetic expression permits to explain the different qualitative results previously reported by Luñak and Sedlák [5].

3. Mass balances

A mass balance for the species (i) in the batch, well-stirred tank photoreactor gives [9]:

$$\frac{\mathrm{d}\langle C_i(\boldsymbol{x}, t)\rangle_{V_{\mathrm{L}}}}{\mathrm{d}t} = \frac{V_{\mathrm{irr}}}{V_{\mathrm{L}}}\langle R_{\mathrm{i}}(\boldsymbol{x}, t)\rangle_{V_{\mathrm{irr}}} = \frac{V_{\mathrm{irr}}}{V_{\mathrm{L}}}\frac{1}{y_{\mathrm{L}}}\int_0^{y_{\mathrm{L}}} R_{\mathrm{i}}(y, t)\mathrm{d}y \tag{21}$$

with the following initial condition:

$$\langle C_{\mathrm{i}}(\boldsymbol{x}, 0)\rangle_{V_{\mathrm{L}}} = C^0_{\mathrm{i}} \tag{22}$$

Since e^a is a irreducible function of position, so is R_{i}. Consequently, an average value of concentrations and reaction rates are necessary. It will be seen below that a one-dimensional model is applicable for e^a. Hence, the average value is taken over the reactor length (y_{L}).

The required reaction rates for the mass balance can be obtained from the kinetic model given by Eq. (14). Substituting the reaction rate for the stable species (i = D, DCP, CHQ and P) into Eq. (21) we finally get

$$\frac{\mathrm{d}C_{\mathrm{D}}}{\mathrm{d}t} = -\frac{V_{\mathrm{irr}}}{V_{\mathrm{L}}}[(\Phi_{\mathrm{D,DCP}} + \Phi_{\mathrm{D,CHQ}})\langle e^a_{\mathrm{D}}\rangle_{y_{\mathrm{L}}} + k_{\mathrm{D,DCP}} C_{\mathrm{D}}\langle (e^a_{\mathrm{P}})^{1/2}\rangle_{y_{\mathrm{L}}} + k_{\mathrm{D,CHQ}} C_{\mathrm{D}}\langle (e^a_{\mathrm{P}})^{1/2}\rangle_{y_{\mathrm{L}}}] \tag{23}$$

$$\frac{\mathrm{d}C_{\mathrm{DCP}}}{\mathrm{d}t} = \frac{V_{\mathrm{irr}}}{V_{\mathrm{L}}}[\Phi_{\mathrm{D,DCP}}\langle e^a_{\mathrm{D}}\rangle_{y_{\mathrm{L}}} - \Phi_{\mathrm{DCP}}\langle e^a_{\mathrm{DCP}}\rangle_{y_{\mathrm{L}}} + k_{\mathrm{D,DCP}} C_{\mathrm{D}}\langle (e^a_{\mathrm{P}})^{1/2}\rangle_{y_{\mathrm{L}}} - k_{\mathrm{DCP,HA}} C_{\mathrm{DCP}}\langle (e^a_{\mathrm{P}})^{1/2}\rangle_{y_{\mathrm{L}}}] \tag{24}$$

$$\frac{\mathrm{d}C_{\mathrm{CHQ}}}{\mathrm{d}t} = \frac{V_{\mathrm{irr}}}{V_{\mathrm{L}}}[\Phi_{\mathrm{D,CHQ}}\langle e^a_{\mathrm{D}}\rangle_{y_{\mathrm{L}}} - \Phi_{\mathrm{CHQ}}\langle e^a_{\mathrm{CHQ}}\rangle_{y_{\mathrm{L}}} + k_{\mathrm{D,CHQ}} C_{\mathrm{D}}\langle (e^a_{\mathrm{P}})^{1/2}\rangle_{y_{\mathrm{L}}} - k_{\mathrm{CHQ,HA}} C_{\mathrm{CHQ}}\langle (e^a_{\mathrm{P}})^{1/2}\rangle_{y_{\mathrm{L}}}] \tag{25}$$

$$\frac{\mathrm{d}C_{\mathrm{P}}}{\mathrm{d}t} = -\frac{V_{\mathrm{irr}}}{V_{\mathrm{L}}}[k_{\mathrm{P1}}\langle e^a_{\mathrm{P}}\rangle_{y_{\mathrm{L}}} + k_{\mathrm{P2}} C_{\mathrm{P}}\langle (e^a_{\mathrm{P}})^{1/2}\rangle_{y_{\mathrm{L}}}] \tag{26}$$

This set of four non-linear, first-order, ordinary differential equations must be numerically solved with the initial conditions given by Eq. (22). Integration of these equations provides the time evolution of the D, DCP, CHQ and P molar concentrations.

4. Volumetric rate of photon absorption

In order to complete the theoretical description of the model, it is necessary to introduce the radiation field expression on the right hand side of the mass balance equations Eqs. (23)–(26). The spectral Local Volumetric Rate of Photon Absorption (e^a_λ) is a function of position ($\boldsymbol{x}$) and time (t):

$$e^a_\lambda = e^a_\lambda(\boldsymbol{x}, t) = e^a_\lambda(y, r, \beta, t) \tag{27}$$

where y, r and β are the axial, radial and angular cylindrical coordinates placed at the bottom and center of the batch, well-stirred tank photoreactor, respectively.

In previous communications, a rigorous radiation field model inside a similar reactor-reflector-lamp system has been proposed and experimentally verified [13–15]. Using a three-dimensional cylindrical coordinate system, the authors found that radial and angular variations were not very significant for a restricted set of geometrical and optical parameters. Thus, the following one-dimensional model can describe the monochromatic LVRPA spatial distribution:

$$e^a_{\mathrm{i}}(y, t) = \kappa_{\mathrm{i}}(t) G_{\mathrm{W}} \exp[-\kappa_{\mathrm{T}}(t) y] \tag{28}$$

where the total absorption coefficient (κ_{T}) is given by

$$\kappa_{\mathrm{T}}(t) = \sum_{\mathrm{j}=1}^{N} \alpha_{\mathrm{j}} C_{\mathrm{j}}(t) \quad (\mathrm{j}: \mathrm{D, DCP, CHQ, P, HA}) \tag{29}$$

Note that for calculating κ_{T}, we have also included the radiation absorption of all intermediate reaction products: 2,4-dichlorophenol (DCP), chlorohydroquinone (CHQ), and humic acids (HA).

Finally, the local values of $e^a_{\mathrm{i}}(y, t)$ for the radiation absorbing species (D, DCP, CHQ and P) must be integrated over the reactor length (recall the one-dimensional model) to obtain the corresponding volume averaged VRPA:

$$\langle e^a_{\mathrm{i}}(y, t)\rangle_{y_{\mathrm{L}}} = \frac{\kappa_{\mathrm{i}}(t)}{\kappa_{\mathrm{T}}(t)} G_{\mathrm{W}} \frac{1}{y_{\mathrm{L}}}\{1 - \exp[-\kappa_{\mathrm{T}}(t) y_{\mathrm{L}}]\} \quad (\mathrm{i} = \mathrm{D, DCP, CHQ, P}) \tag{30}$$

A similar procedure is used to evaluate the volume average of the square root of the VRPA for the case of hydrogen peroxide (P):

$$\langle [e^a_{\mathrm{P}}(y, t)^{1/2}]\rangle_{y_{\mathrm{L}}} = \frac{[\kappa_{\mathrm{P}}(t) G_{\mathrm{W}}]^{1/2}}{\kappa_{\mathrm{T}}(t)} \frac{2}{y_{\mathrm{L}}} \times \left\{1 - \exp\left[-\frac{\kappa_{\mathrm{T}}(t) y_{\mathrm{L}}}{2}\right]\right\} \tag{31}$$

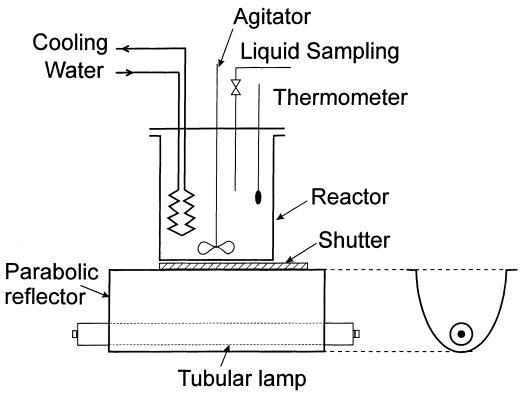

Fig. 2. Schematic diagram of the stirred tank photoreactor.

5. Experiments

5.1. Apparatus and operating conditions

The employed apparatus is described in Fig. 2. The equipment is made of: (1) a perfectly mixed isothermal tank reactor; (2) an irradiating system that consists of a 15 W, low Hg pressure, low output power, Germicidal tubular lamp, with emission at 253.7 nm, placed at the focal axis of a cylindrical reflector of parabolic cross-section; (3) a system for measuring and controlling the reaction temperature; and (4) a sampling device. Table 2 presents a summary of the principal reactor, reflector and lamp characteristics. Note that the irradiated volume of solution (V_{irr}) was calculated as the product of the irradiated area (A_{irr}) and the liquid height (y_L) of the reactor and that the irradiated area is not exactly equal to the total area of the cylindrical reactor.

Operating conditions were as follows: (i) the initial molar ratio of hydrogen peroxide/2,4-D was varied from 0 to 16 (nominal); (ii) the initial 2,4-D concentration was varied from 30 to 90 ppm; and (iii) temperature was kept constant at 293 K.

Table 2
Reactor, reflector and lamp characteristics

Reactor	
Volume	2000 cm^3
Irradiated area	132.7 cm^2
Liquid height	12.6 cm
Irradiated volume	1672 cm^3
Reflector	
Parabola characteristic constant	2.1 cm
Distance vertex of parabolic reflector — reactor plate	8.4 cm
Length	15.8 cm
LAMP G15T8 (almost monochromatic)	
Nominal power	15 W
Output power at 253.7 nm (nominal)	3.6 W
Diameter	2.54 cm
Nominal length[a]	44.72 cm

[a] Note that, according to the size of the reflector, no more than 15.8 cm of this lamp are used in the reacting system. In this way, lamp end effects are totally excluded, but the nominal output power actually used is very much smaller than 3.6 W.

5.2. Materials and procedure

The reactant was purified by dissolution in benzene and subsequent crystallization (two times) achieving a purity of 99% compared with an EPA standard (# 2940, 99.78%). Hydrogen peroxide was 30.4% (p/v).

Prior to each run the reactor temperature and the lamp operation must reach steady state. A shutter located between the illuminating system and the reactor bottom allows to obtain the specified operating conditions. Then, the shutter can be removed and the reaction starts. Temperature was controlled with the aid of a cryostat (Lauda K4R) and the lamp operating conditions with a V-A-W meter (Clarke Hess, 255).

Runs were carried out during 6 h and samples were taken at different time intervals according to the course of the reaction (shorter intervals during the first 2 h and longer ones afterwards). For each experimental run the total volume of the different samples taken for analysis never exceeded 10% of the total initial reaction volume. Organic compounds were analyzed with HPLC (Perkin Elmer with UV–VIS detector) following the procedure recommended by Coonick and Simoneaux [16]. A TOC analyzer (Shimadzu TOC-5000A) was used in parallel to monitor the amount of organic matter that was being totally destroyed (mineralized). The optical properties of the reacting system were also spectrophotometrically analyzed in each sample by getting absorbance measurements at 253.7 nm (UV–VIS Cary 17D). Hydrogen peroxide concentration was measured according to Allen et al. [17], employing the same spectrophotometer at 350 nm. The pH of each sample was also controlled.

6. Experimental results

Fig. 3 shows some experimental results for a 2,4-D initial concentration of 30 ppm. The initial H_2O_2/2,4-D molar ratios were $r = 0$, 1.1, 6.8 and 15.8. Plots indicate: (i) 2,4-D concentration; (ii) H_2O_2 concentration; and (iii) concentration of the most important reaction intermediates. Two of the most important, well-defined reaction intermediates included in the simplified reaction path (CHQ and DCP) have been clearly detected.

It is observed that addition of hydrogen peroxide increases significantly the degradation rate of 2,4-D when compared with the application of direct photolysis exclusively ($r = 0$). Under the adopted operating conditions, initial degradation rates twenty times greater than those obtained employing only UV radiation may be observed.

Fig. 4 shows experimental results indicating changes in TOC for the same reaction times and for three different initial 2,4-D concentrations: 30, 60 and 90 ppm. The same

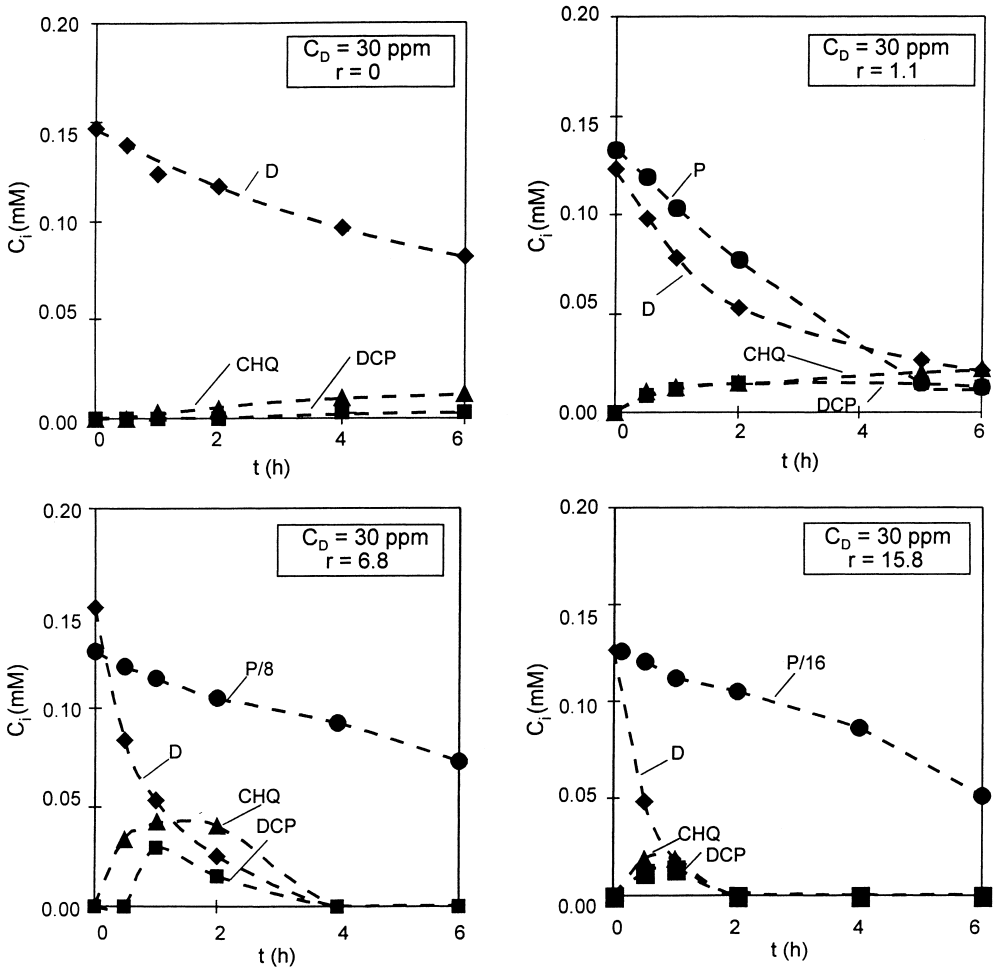

Fig. 3. Concentration vs. time experimental results for $C_D^0 = 30$ ppm and $r = 0$, 1.1, 6.8 and 15.8.

nominal, initial concentration ratios as before were employed ($r = 0$, 1, 8, and 16). It was found that, TOC conversion is larger at lower initial 2,4-D concentrations and increases when r becomes higher. For example, for an initial 2,4-D concentration of 60 ppm, TOC conversions after 6 h of reaction, are 8.2, 8.3, 51.0 and 55.8% for $r = 0$, 1.0, 6.6 and 16.4, respectively.

It was indicated before that the 2,4-D photooxidation generates intermediate reaction products that are equally toxic than the original reactant. Results as those reported in Fig. 4 have the advantage of showing the real decrease of water pollutant concentrations in the system regardless of the individual compositions. It can be noted, for example that, with $C_{2,4\text{-D}}^0 = 30$ ppm and $r = 15.8$, after 6 h of

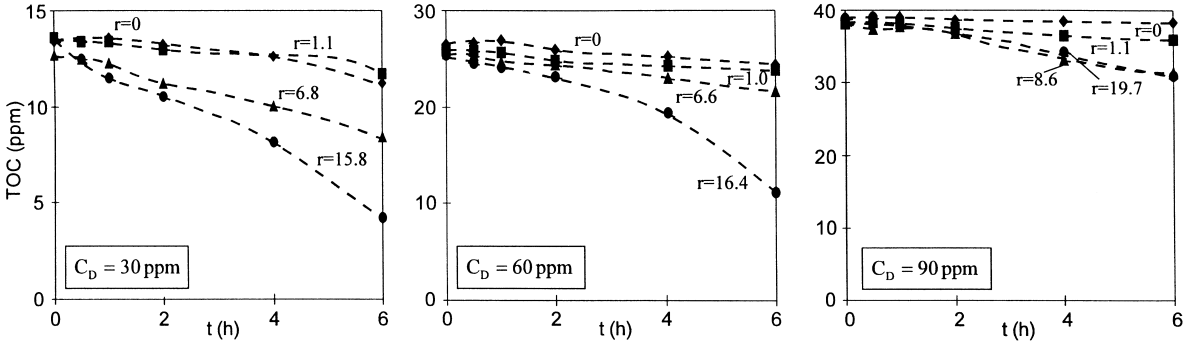

Fig. 4. Experimental results of TOC vs. time for $C_D^0 = 30$, 60 and 90 ppm.

reaction, the reduction of the "total contaminant concentration" is about 70%, in spite that the concentration of 2,4-D and the two main reaction intermediates has fallen to almost zero. Employing this low output power lamp most of this organic content is attributable to humic acids that are normal constituents of natural waters; i.e. no harms should be expected from these compounds. However, with higher powered lamps and higher hydrogen peroxide concentrations, one should expect that humic acids will further decompose to render complete mineralization to carbon dioxide and water.

7. Kinetic parameters evaluation

Using the experimental results of the previous section, we applied regression parameter estimation methods to obtain the kinetic constants of the system. Obviously, this result will also indicate those effects associated with the optical properties of the reacting system and their influence on the functional dependence of the reaction rates with respect to the LVRPA.

Steps 1–6 in Table 1 correspond to a widely accepted reaction mechanism for the interaction of UV radiation with hydrogen peroxide. CHQ, DCP and humic acids are well known reaction intermediates. Finally, steps 7 and 8 correspond to the $OH^{\bullet}$ attack on the different hydrocarbons present in the reaction sequence described in Fig. 1 (cf. Luñak and Sedlák [5]). Therefore, it was considered that no model discrimination studies were needed.

According to the kinetic model represented by Eq. (14), we have ten unknowns: four direct photolysis quantum yields ($\Phi_{D,DCP}$, $\Phi_{D,CHQ}$, Φ_{DCP}, and Φ_{CHQ}) and six kinetic parameters for the reaction with hydrogen peroxide and UV radiation ($k_{D,DCP}$, $k_{D,CHQ}$, $k_{DCP,HA}$, $k_{CHQ,HA}$, k_{P1}, and k_{P2}). In addition, Eq. (29) needs five molar absorptivities (α_j: j = D, DCP, CHQ, P and HA). Quantum yields and molar absorptivities have been obtained from independent experiments.

7.1. Molar absorption coefficients

Standard measurements in a Cary 17D, UV–VIS, double beam spectrophotometer can be used to obtain the molar absorption coefficients at 253.7 nm for DCP, CHQ and P reacting species. The absorption coefficient for 2,4-D (α_D) at 253.7 nm can be obtained from Cabrera et al. [9]. On the other hand, a straightforward extension of a previously developed method for obtaining the molar absorptivity of humic acids (α_{HA}) at the same wavelength was used [9]. It provides α_{HA} as a function of the properties of all the other compounds detected in the solution; i.e. the concentration of humic acids was obtained by difference between the initial values of the 2,4-D concentration and the actual concentrations of 2,4-D, CHQ and DCP.

Table 3
Values of the molar absorption coefficients

Molar absorption coefficient	Value ($cm^2\ mol^{-1}$)
α_D	0.409×10^6
α_{DCP}	0.464×10^6
α_{CHQ}	0.608×10^6
α_{HA}[a]	0.414×10^7
α_P	0.368×10^5

[a] Empirical correlation.

Values of the five molar absorption coefficients are indicated in Table 3.

7.2. Direct photolysis quantum yields

In a previous work [9] we have presented a methodology to evaluate the kinetic parameters for the photodecomposition of 2,4-D from a proposed kinetic model and the concentration versus time experimental data. Here, we will use a similar procedure for obtaining the direct photolysis quantum yields of D, DCP and CHQ reacting species.

Experimental runs for each one of the organic compounds were performed in the same batch, well-stirred tank photoreactor. In these studies, three different initial concentrations of the reacting species (D, DCP or CHQ) were employed. Then, making use of the experimental concentration versus time data and a non-linear regression procedure, the direct photolysis quantum yields at 253.7 nm can be obtained.

Within the range of the initial concentrations of the reacting species used along this kinetic study, the direct photolysis quantum yields are independent of the corresponding initial concentrations. Table 4 gives the values of the four quantum yields obtained with the regression program for each separated direct photolysis reaction: $\Phi_{D,DCP}$, $\Phi_{D,CHQ}$, Φ_{DCP}, and Φ_{CHQ}.

7.3. Kinetic parameters for the H_2O_2/UV reaction

In order to calculate the kinetic parameters for the H_2O_2/UV reaction, a numerical method was used. It was a direct application of a non-linear least square method to

Table 4
Numerical values for the kinetic constants

Kinetic constant	Units	Values
$\Phi_{D,DCP}$	mol einstein^{-1}	0.0107
$\Phi_{D,CHQ}$	mol einstein^{-1}	0.0024
Φ_{DCP}	mol einstein^{-1}	0.0184
Φ_{CHQ}	mol einstein^{-1}	0.0426
$k_{D,DCP}$	$(cm^3\ einstein^{-1}\ s^{-1})^{1/2}$	8.23
$k_{D,CHQ}$	$(cm^3\ einstein^{-1}\ s^{-1})^{1/2}$	14.91
$k_{DCP,HA}$	$(cm^3\ einstein^{-1}\ s^{-1})^{1/2}$	58.26
$k_{CHQ,HA}$	$(cm^3\ einstein^{-1}\ s^{-1})^{1/2}$	24.90
k_{P1}	mol einstein^{-1}	0.609
k_{P2}	$(cm^3\ einstein^{-1}\ s^{-1})^{1/2}$	1.63×10^{-5}

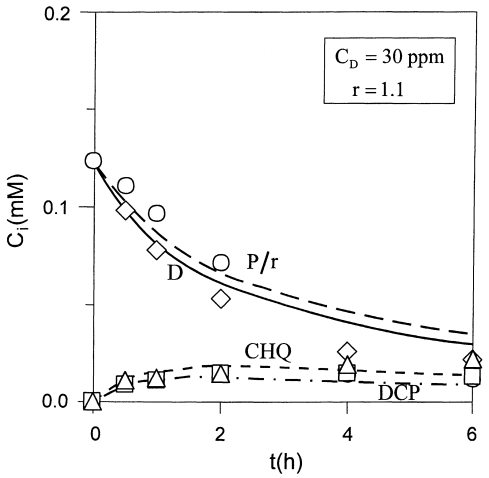

Fig. 5. Model and experimental concentrations vs. time for $C_D^0 = 30$ ppm and $r = 1.1$. Keys: (◇, ——) 2,4-dichlorophenoxyacetic acid; (○, — —) hydrogen peroxide; (△, - - -) chlorohydroquinone; and (□, –·–·–) 2,4-dichlorophenol.

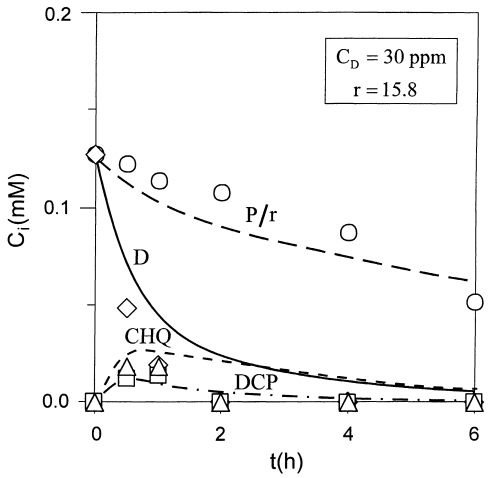

Fig. 7. Model and experimental concentrations vs. time for $C_D^0 = 30$ ppm and $r = 15.8$. Keys: (◇, ——) 2,4-dichlorophenoxyacetic acid; (○, — —) hydrogen peroxide; (△, - - -) chlorohydroquinone; and (□, –·–·–·–) 2,4-dichlorophenol.

minimize the sum of the squares of the differences between experimental and calculated concentrations, the last one obtained from the kinetic model. This calculation was carried out employing all experimental runs, i.e. all analyzed chemical species concentrations and all the corresponding sample times. In order to obtain the model predictions, a special subroutine must calculate the concentrations of the four species (D, CHQ, DCP and P) by solving the system of four ordinary, non-linear differential equations defined by Eqs. (22)–(26). An implicit Runge–Kutta formula was used.

Figs. 5–7 show the experimental data and model predictions as a function of time for a 2,4-D initial concentration of 30 ppm. Plots indicate the molar concentrations of the following reacting species: 2,4-D, H_2O_2 (divided by the corresponding molar ratio, r), DCP, and CHQ. The initial H_2O_2/2,4-D molar ratios were: $r = 1.1$ (Fig. 5), $r = 6.8$ (Fig. 6) and $r = 15.8$ (Fig. 7).

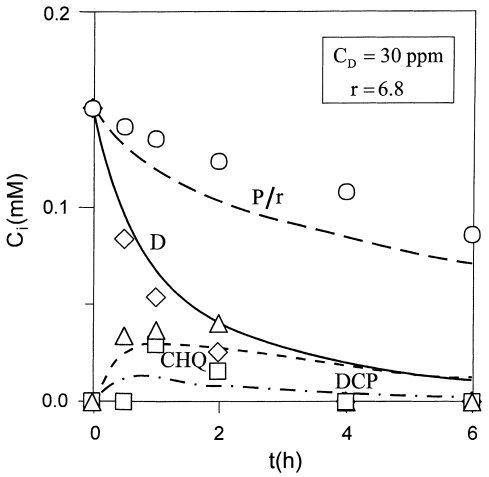

Fig. 6. Model and experimental concentrations vs. time for $C_D^0 = 30$ ppm and $r = 6.8$. Keys: (◇, ——) 2,4-ducichlorophenoxyacetic acid; (○, — —) hydrogen peroxide; (△, - - -) chlorohydroquinone; and (□, –·–·–) 2,4-dichlorophenol.

When the mixture under analysis is made up of compounds having very dissimilar concentrations (cf. 2,4-D and H_2O_2 versus CHQ and DCP) the method tends to give larger errors in the prediction of the concentration evolution of the second group of components. This problem can be observed in Figs. 5–7. Moreover, when the concentration of humic acids become important, all problems related to their correct quantification becomes increasingly influential in the prediction of the results. These considerations being taken into account, fairly good agreement between model predictions and experimental data can be observed. Only for low experimental concentrations of the reacting species, namely lower than ≈0.05 mM, the relative error is sometimes significant. On the contrary, for molar concentrations higher than this value, the maximum deviation is not larger than 20%.

Table 5 provide statistical figures of merit for the estimated kinetic constant for 95 and 65% confidence interval (CI). These results, on the light of the difficulties associated with this particular chemical system seem acceptable.

Table 5
Errors for standard confidence intervals

Kinetic constant	Estimated value	95% (CI)	65% (CI)
$k_{D,DCP}$	8.23	3.93	1.86
$k_{D,CHQ}$	14.91	4.05	1.92
$k_{DCP,HA}$	58.26	15.78	7.48
$k_{CHQ,HA}$	24.90	13.97	6.62
k_{P1}	0.609	0.146	0.0691
k_{P2}	$1.63 \times 10^{-5} \cong 0$	–	–

Table 6
Parametric sensitivity, finite difference approximation

Modified kinetic constant	% change in 2,4-D predicted conversion with a 10% change in the value of the kinetic constant	% change in 2,4-D predicted conversion with a 25% change in the value of the kinetic constant
$k_{D,DCP}$	2.6	6.5
$k_{D,CHQ}$	4.8	11.9
$k_{DCP,HA}$	0.4	0.9
$k_{CHQ,HA}$	0.4	0.9
k_{P1}	0.9	2.3
k_{P2}	≅0	≅0

7.4. Parametric sensitivity

Based on a sensitivity analysis using the finite difference technique proposed by Wu et al. [18], we have defined our sensitivity problem as the maximum variation that experiments the prediction of the 2,4-D conversion along the degradation reaction when some of the kinetic parameters (rate constants) are subjected to a given change. Each one of the kinetic parameter reported in Table 4, was separately modified in its value by 10 and 25%, respectively (the values of the other kinetic constants were kept constant). Results are illustrated in Table 6. The maximum deviation (11.9%) was observed when the second kinetic constant was changed by 25%. It can be concluded that the described kinetic model is not very sensitive to changes in the obtained kinetic parameters and that the maximum sensibility appears with changes in the kinetic constant corresponding to the reaction that transforms 2,4-D into CHQ.

Additional studies to investigate the existence of an optimal hydrogen peroxide/2,4-D concentration ratio and the effect of employing lower radiation wavelengths are underway.

8. Conclusions

The main conclusions can be summarized as follows:

- Compared with direct photolysis, addition of hydrogen peroxide to the studied reaction increases significantly the degradation rate of the 2,4-dichlorophenoxyacetic acid (2,4-D). Under the studied conditions, a reaction rate twenty times greater has been obtained.
- Immediately after the initiation of the degradation reaction, equally toxic intermediate products such as 2,4-dichlorophenol (DCP) and chlorohydroquinone (CHQ) can be detected. However, since the system was also studied including a parallel evaluation of the total organic carbon (TOC), it is possible to reach more useful conclusions concerning the ability of the H_2O_2/UV system to reduce the initial contamination to innocuous final products.
- TOC percentage reduction is larger at low 2,4-D initial concentrations and increases significantly when the initial H_2O_2/2,4-D ratio is higher. After 6 h of operation for $C^0_{2,4\text{-D}} = 30$ ppm, a reduction of total contamination up to 70% has been achieved.
- A kinetic model has been developed to describe the degradation of 2,4-D using hydrogen peroxide plus UV radiation. The kinetic representation exhibits, as limiting cases, the following H_2O_2 reaction rate features: (i) for low photon absorption rates: a linear dependence with respect to the H_2O_2concentration and a square root dependence with respect to the LVRPA and (ii) for high photon absorption rates: a zero-order dependence with respect to the H_2O_2concentration and a linear dependence with respect to the LVRPA.
- The kinetic parameters were obtained from the experimental data by application of the model to the whole time evolution of the H_2O_2/UV reaction. When predictions of the kinetic model are compared with experimental results, a reasonable representation of the 2,4-D, H_2O_2, CHQ and DCP concentration evolution for a rather wide range of their initial concentrations is obtained.
- For predicting the 2,4-D degradation, the parametric sensitivity corresponding to significant variations in the obtained values of the different kinetic constants resulting from the model is very low.

Acknowledgements

The authors are grateful to Consejo Nacional de Investigaciones Científicas y Técnicas (CONICET), Universidad Nacional del Litoral (UNL), Agencia Nacional de Promoción Científica y Tecnológica (ANPCyT) and Programa de Modernización Tecnológica-SECyT-CONICET (PID 22), for their support to produce this work. They also thank Dr. M.I. Cabrera for her helpful comments about the kinetic model, Lic. M.J. Martínez and Tec. E.M. Ruiz for their valuable help in the experimental work, and Eng. C.M. Romani for technical assistance.

References

[1] C.-R. Huang, H.-Y. Shu, The reaction kinetics, decomposition pathways and intermediate formations of phenol in ozonation, UV/O_3 and UV/H_2O_2 process, J. Hazard. Mater. 42 (1995) 47–64.

[2] D.G. Hager, UV-catalyzed hydrogen peroxide chemical oxidation of organic contaminants in water, in: H.M. Freeman (Ed.), Physical Chemical Processes, Vol. 2, Cincinnati, OH, 1990, pp. 143–153.
[3] L. Plant, M. Jeff, Hydrogen peroxide: a potent force to destroy organics in wastewater (Chem. Eng. 1994) 16–20.
[4] E. Froelich, Advanced chemical oxidation of contaminated water using the perox-pure oxidation system, in: W.W. Eckenfelder, A.R. Bowers, J.A. Roth (Eds.), Chemical Oxidation, Nashville, Tennessee, 1991, pp. 104–113.
[5] S. Luñák, P. Sedlák, Photoinitiated reactions of hydrogen peroxide in the liquid phase, J. Photochem. Photobiol. A: Chem. 68 (1992) 1–33.
[6] P. Pichat, J.-C. D'Oliveira, J.-F. Maffre, D. Mass, Destruction of 2,4-dichlorophenoxyethanoic acid (2,4-D) in water by TiO_2-UV, H_2O_2-UV or direct photolysis, in: D.F. Ollis, H. Al-Ekabi (Eds.), Photocatalytic Purification and Treatment of Water and Air, 1993, pp. 683–688.
[7] C. Scheuer, B. Wimmer, H. Bischof, L. Nguyen, J. Maguhn, P. Spitzauer, A. Kettrup, D. Wabner, Oxidative decomposition of organic water pollutants with UV-activated hydrogen peroxide. Determination of anionic products by ion chromatography, J. Chromat. A 706 (1995) 253–258.
[8] B. Wimmer, H. Bischof, C. Scheuer, D. Wabner, Oxidative degradation of organic pollutants-products and reaction pathways, Vom Wasser 85 (1995) 421–432.
[9] M.I. Cabrera, C.A. Martín, O.M. Alfano, A.E. Cassano, Photochemical decomposition of 2,4-dichlorophenoxyacetic acid in aqueous solution. I. Kinetic study, Water Sci. Technol. 35 (1997) 31–39.
[10] D.E. Lea, The termination reaction in the photolysis of hydrogen peroxide in dilute aqueous solutions, Trans. Faraday Soc. 45 (1949) 81–85.
[11] J. Weiss, The free radical mechanism in the reactions of hydrogen peroxide, in: W.G. Frankenburg, V.I. Konarewsky, E.K. Rideal (Eds.), Advances in Catalysis, Vol. 4, Academic Press, New York, 1952, pp. 343–365.
[12] F.S. Dainton, J. Rowbottom, The primary radical yield in water. A comparison of the photolysis and radiolysis of solutions of hydrogen peroxide, Trans. Faraday Soc. 49 (1953) 1160–1173.
[13] O.M. Alfano, R.L. Romero, A.E. Cassano, A cylindrical photoreactor irradiated from the bottom. I. Radiation flux density generated by a tubular source and a parabolic reflector, Chem. Eng. Sci. 40 (1985) 2119–2127.
[14] O.M. Alfano, R.L. Romero, A.E. Cassano, A cylindrical photoreactor irradiated from the bottom. II. Models for the local volumetric rate of energy absorption with polychromatic radiation and their evaluation, Chem. Eng. Sci. 41 (1986) 1155–1161.
[15] O.M. Alfano, R.L. Romero, C.A. Negro, A.E. Cassano, A cylindrical photoreactor irradiated from the bottom. III. Measurement of absolute values of the local volumetric rate of energy absorption. Experiments with polychromatic radiation, Chem. Eng. Sci. 41 (1986) 1163–1169.
[16] W.J. Coonick, J.M. Simoneaux, Determination of (2,4-dichlorophenoxy) acetic acid and 2,6-dichlorobenzonitrile in water by high-performance liquid chromatography, J. Agric. Food. Chem. 30 (1982) 258–260.
[17] A.O. Allen, C.J. Hochanadel, J.A. Ghormley, T.W. Davis, Decomposition of water and aqueous solutions under mixed fast neutron and gamma radiation, J. Phys. Chem. 56 (1952) 575–586.
[18] H. Wu, R. Rota, M. Morbidelli, A. Varma, Parametric sensitivity in fixed-bed catalytic reactors with reverse-flow operation, Chem. Eng. Sci. 54 (1999) 4579–4588.